Interpretation of charged-particle spectra in $p + p$ and $p + \mathrm{Pb}$ collisions at energies available at the CERN Large Hadron Collider using an improved HIJING code with a collective cascade

Khaled Abdel-Waged* and Nuha Felemban

Department of Physics, Faculty of Applied Science, Umm Al-Qura University, P.O. Box (10471), Makkah, Saudi Arabia

(Received 24 December 2014; revised manuscript received 23 February 2015; published 30 March 2015)

We supplement the Heavy Ion Jet Interaction Generator (HIJING) code with a collective cascade recipe and updated Martin-Stirling-Thorne-Watt (MSTW2009) parton distribution functions (PDFs) to describe nonsingle diffractive (NSD) $p + p$ and Pb collisions at CERN Large Hadron Collider energies. The collective cascade, developed in the space of an impact parameter, is used to induce nuclear modification of nucleons, that are involved in primary interactions, inside the dense nuclear medium. It is found that the improved HIJING (ImHIJING) code (that with MSTW2009 PDFs) reproduces rather well the pseudorapidity density, the multiplicity, and the transverse momentum distributions of charged particles within the pseudorapidity interval $|\eta_{\mathrm{c.m.system}}| < 2.4$ in NSD $p + p$ collisions at $\sqrt{s_{\mathrm{NN}}} = 0.9$, 2.36, and 7 TeV. The ImHIJING with collective cascade calculations is also shown to be a good fit to the pseudorapidity density (in the laboratory system) and transverse momentum (p_T) dependence of the nuclear modification of charged particles in NSD $p + \mathrm{Pb}$ collisions at $\sqrt{s_{\mathrm{NN}}} = 5.02$ TeV. The effects of the collective cascade are clearly seen in the target ($3 < \eta_{\mathrm{lab}} < 4$) and central (within $|\eta_{\mathrm{c.m.system}}| < 0.3$ at $1 < p_T < 8$ GeV/c) interaction regions when studying the pseudorapidity density and transverse momentum dependence of the nuclear modification factor of the charged particles, respectively.

DOI: 10.1103/PhysRevC.91.034908 PACS number(s): 13.85.−t, 13.75.Cs, 25.40.−h, 24.10.Jv

I. INTRODUCTION

Charged particles produced at high transverse momentum ($p_T \geqslant 1$ GeV/c) in proton-nucleus ($p + A$) and nucleus-nucleus ($A + A$) collisions at CERN Large Hadron Collider (LHC) energies are important observable for the study of nuclear effects [1–4]. It is shown that these particles are suppressed compared to the expectation from independent binary nucleon-nucleon (NN) collisions. Such high p_T-particles' suppression provides critical tests of models that describe quantum chromodynamic matter (QCD) at high gluon densities.

A successful attempt for the description of particles' production in proton-proton ($p + p$), $p + A$, and $A + A$ collisions from Relativistic Heavy Ion Collider (RHIC) to LHC energies has been the Heavy Ion Jet Interaction Generator (HIJING) model [5,6]. The model is based on a two component geometrical model of hard (with minijet production) and soft interactions. The hard component is characterized by a momentum transverse larger than a cutoff scale (p_0) and is evaluated by perturbative QCD (pQCD) using the parton distribution function (PDF) in a nucleon. On the other hand, the soft component ($p_T < p_0$) takes into account the non-pQCD, is characterized by a soft parton cross section (σ_{soft}), and is modeled by the formation and fragmentation of quark-gluon strings. For $p + A$ and $A + A$ collisions, the HIJING implements nuclear effects via nuclear modification of the parton distributions functions (so-called parton shadowing) which are shown to influence the flux of partons and, in turn, to the description of charged particles [6].

Although the HIJING provides an adequate description of RHIC and LHC data, especially for $p + p$ collisions, a systematic disagreement is found when trying to describe simultaneously the pseudorapidity density and transverse momentum dependence of the nuclear modification factor of charged particles in nonsingle diffractive (NSD) $p + \mathrm{Pb}$ collisions at $\sqrt{s_{\mathrm{NN}}} = 5.02$ TeV [1,4,7]. Possible causes are the implementation of relatively old Gluck-Reya-Vogt (GRV1995) parametrizations of PDFs [8] and the neglect of nucleon shadowing in the initial states of the interactions.

In this paper, we introduce an improved version of the HIJING (ImHIJING) in which we use more modern sets of Martin-Stirling-Thorne-Watt (MSTW2009) PDFs [9]. Nuclear effects are treated in the ImHIJING by utilizing a collective cascade recipe [10,11], which basically amounts to a cascade in the two-dimensional space of a projected radius vector of target nucleons on a plane perpendicular to the momentum of the projectile proton (on the plane of the impact parameter) with a cascade power independent of produced particles (see Fig. 1). The collective cascade induces nuclear modification of nucleons, that are involved in the primary interactions, inside the target nucleus. In particular, nucleons taking part in the primary interactions suffer energy loss due to cascading with other noninteracting ones, and the remaining energy is used to produce jets or excited strings according to the HIJING model. Such nucleon shadowing is expected to influence the description of high p_T-charged particles, especially in the regions of space where the density of the nuclear medium is high. It should be noted that the collective cascade picture introduced here is also used in the modified FRITIOF model [12] to solve the problem of slow particles' spectra ($p_T < 1$GeV/c), that are involved in the rescattering process by knocking out further nucleons while cascading into the nucleus [13,14].

This article is organized as follows: Sec. II defines the basic ingredients of the ImHIJING plus a collective cascade model. In Sec. III, we apply the model systematically to the charged particles' spectra in NSD $p + p$ and $p + \mathrm{Pb}$ collisions at LHC energies. We summarize and conclude this paper in Sec. IV.

*khelwagd@yahoo.com

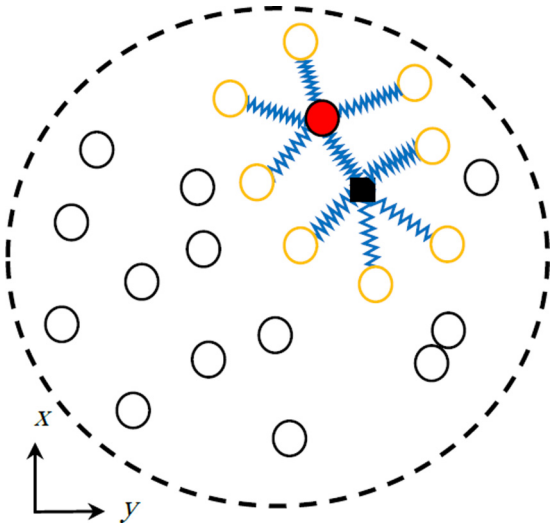

FIG. 1. (Color online) A schematic of the Regge collective cascade for a single $p + A$ collision on the impact-parameter plane. All nucleons are shown as open circles, a primary interacting nucleon is marked by the closed circle, the set of individual Reggeon exchanges is marked by the wavy lines, and the square point is the Reggeon interaction vertex.

II. DESCRIPTION OF THE HIJING MODEL WITH COLLECTIVE CASCADING

Here, we describe an outline of the improved HIJING model. Details of the HIJING are described in Ref. [5].

All HIJING-type models [5,6,15,16] describe the interactions of protons with nuclei as binary collisions between a primary particle and an individual nucleon of the nucleus. At a given impact parameter ($\vec{b}$) and given center-of-mass energy ($\sqrt{s}$), NN scatterings are handled by the eikonal formalism. Particles produced from two colliding nucleons at high energies ($\sqrt{s} > 4$ GeV) are described by a hard and a soft component. The hard component involves processes in which minijets are produced with transverse momentum p_T larger than a transverse momentum cutoff p_0. The inclusive cross section $\sigma_{\rm jet}$ of the minijets is described by perturbative QCD, which depends on the parton-parton cross section σ_{ab}, parton distribution function $f_{a(b)}(x_{a(b)}, Q^2)$, and p_0, where $x_{a(b)}$ is the light-cone fraction momentum of parton $a(b)$. The kinematics of the jets and the associated initial- and final-state radiations are simulated by the PYTHIA model [17]. On the other hand, the soft component ($p_T < p_0$), characterized by a soft cross section $\sigma_{\rm soft}$, treats nonperturbative processes and is modeled by the formation and fragmentation of strings along the lines of the FRITIOF [12] and the dual parton model [18,19] models. Both p_0 and $\sigma_{\rm soft}$ are free parameters of the model and are chosen to fit $p + p(\bar{p})$ total cross sections and the (pseudo) rapidity density of charged particles at mid-(pseudo) rapidity.

In the HIJING (version 1.383) [5] the Duke-Owens (DO1984) [20] parametrizations of PDFs are used to fit the experimental $p + p$ and $p + \bar{p}$ data in the energy range of $20 < \sqrt{s_{\rm NN}} < 1800$ GeV using a constant cutoff $p_0 = 2\,{\rm GeV}/c$ and a soft cross section $\sigma_{\rm soft} = 57$ mb, independent of the colliding energy. However, for $p + A$ and $A + A$ collisions at higher LHC energies, e.g., at $\sqrt{s_{\rm NN}} \geqslant 2$ TeV, when minijet production reaches a very small x region of parton distribution, a set of universal PDFs should be used, which incorporates global fits to all available deep inelastic-scattering and related hard-scattering data. The analysis of the recent experimental data shows that the gluon distribution in a nucleon is higher than the DO1984 parametrizations at small x, and therefore the authors of the HIJING assume an energy dependence of the cutoff parameter $p_0(\sqrt{s})$ and a soft cross section $\sigma_{\rm soft}(\sqrt{s})$ in order not to violate the geometrical limit for the total number of minijets per unit transverse area [6]. In the updated version of HIJING 2.0, the GRV1995 [8] parametrizations of PDFs are used where gluon distributions in these PDFs are higher than those of the DO1984 parametrizations. In order to better describe $p + p$ and $A + A$ data from RHIS to LHC using the GRV1995 parametrizations, the energy dependence of the cutoff parameter and soft cross sections are taken as [6]

$$p_0(\sqrt{s}) = 2.62 - 1.084\ \ln(\sqrt{s}) + 0.299\ln^2(\sqrt{s}) - 0.0292\ln^3(\sqrt{s}) + 0.001\,51\ln^4(\sqrt{s}), \quad (1)$$

$$\sigma_{\rm soft}(\sqrt{s}) = 55.316 - 4.1126\ \ln(\sqrt{s}) + 0.854\ln^2(\sqrt{s}) - 0.0307\ln^3(\sqrt{s}) + 0.003\,28\ln^4(\sqrt{s}). \quad (2)$$

In the energy range considered in this paper $0.9 \leqslant \sqrt{s} \leqslant 7$ TeV, the energy dependence of $p_0(\sqrt{s})$ ranges from 3.12 to 5.5 GeV/c. For $\sigma_{\rm soft}(\sqrt{s})$, the corresponding values are 64.04 mb at $\sqrt{s} = 0.9$ TeV and 84.52 mb at $\sqrt{s} = 7$ TeV.

In this paper, we will couple the HIJING with a new global set of the MSTW2009 [9] PDFs, which are prepared in a form of grids and interpolation. Compared to the DO1984 and GRV1995 parametrizations, the MSTW2009 includes global fits to a larger number of data sets, which includes both old and new types of data. The old data are improved in their precision and kinematic range. The new data include the most precise data of inclusive jet production from both HERA and Run II at the Tevatron from the CDF Collaboration [21] and the DØ Collaboration [22,23], that goes to larger jet p_T values. These data are important as they constrain the gluon (and quark) distributions in the domain $0.01 \leqslant x \leqslant 0.5$ [9].

Using the MSTW2009 tabulated form of PDFs and following the same procedure as in HIJING 2.0, we find that the recent experimental data of $p + p$ inelastic and total cross sections at LHC energies [24,25] are fitted (see Table I) by the parametrized energy dependence cutoff scale in the form

$$p_0(\sqrt{s}) \approx 0.7(\sqrt{s})^{0.241}, \quad (3)$$

TABLE I. Values of the $p + p$ inelastic ($\sigma_{\rm in}$) and total ($\sigma_{\rm tot}$) cross sections at LHC energies calculated for both HIJING 1.0 and IMHIJING.

$\sqrt{s}$ (TeV)	HIJING 1.0		IMHIJING	
	$\sigma_{\rm in}$ (mb)	$\sigma_{\rm tot}$ (mb)	$\sigma_{\rm in}$ (mb)	$\sigma_{\rm tot}$ (mb)
0.9	51.00	66.09	50.59	65.43
2.36	60.46	81.70	59.87	80.70
5	70.28	98.55	65.51	90.29
7	74.77	106.4	68.82	96.01

with the soft cross section obtained by Eq. (2). The cutoff scale in Eq. (3) ranges from 3.6 GeV/c at $\sqrt{s} = 0.9$ TeV to 5.9 GeV/c at $\sqrt{s} = 7$ TeV, which is slightly larger than obtained in Eq. (1). The increasing cutoff as required by the data may be taken as indirect evidence of gluon shadowing at very small x inside a proton in $p + p$ collisions at the LHC energies.

One of the main uncertainties in HIJING 1.383 model is the nuclear modification factor of parton distribution functions. It is assumed that the parton distributions in a nucleus (with mass number A), $f_{a/A}(x_a, Q^2)$ are factorizable into parton distributions in a nucleon $f_{a/N}(x_a, Q^2)$ and the parton a shadowing factor $R_{a/A}(x_a)$,

$$f_{a/A}(x_a, Q^2) = R_{a/A}(x_a) f_{a/N}(x_a, Q^2). \tag{4}$$

In the standard HIJING 1.383 calculations, the shadowing effect for quarks (q) and gluons (g) is taken as the same, and the impact-parameter-dependent but Q^2-independent parametrization is given by [5]

$$\begin{aligned} R_{a/A}(x_a,b) &= \frac{f_{a/A}(x_a, Q^2)}{f_{a/N}(x_a, Q^2)} \\ &= 1 + 1.19 \ln^{1/6} A\left[x_a^3 - 1.2\, x_a^2 + 0.21 x_a\right] \\ &\quad - \alpha_a(b)(A^{1/3}-1)\left[1 - \frac{10.8}{\ln(A+1)}\sqrt{x_a}\right] e^{-x_a^2/0.01}. \end{aligned} \tag{5}$$

The impact-parameter dependence of the nuclear shadowing effect is controlled by [5]

$$\alpha_a(b) = \alpha_a \tfrac{4}{3}\sqrt{1 - b^2/R_A^2}, \tag{6}$$

where R_A is the radius of the nucleus $\alpha_a = \alpha_q = \alpha_g = 0.1$. This constraint on quark (gluon) shadowing is model dependent. For example, starting from HIJING 2.0 [6,15], a weaker A parametrization $(A^{1/3} - 1)^{0.6}$ and much stronger impact parameter dependence of the gluon $\alpha_g = 0.17 - 0.28$ are used in order to fit the LHC data [1,7].

The Fermi motion and collective Regge cascading [10,11] are implemented in HIJING 1.383 as follows:

(i) Nucleon coordinates of the target nucleus $(\vec{r}_i, \ldots, \vec{r}_A)$ are simulated by using the default three-parameter Woods-Saxon distribution.

(ii) The Fermi motion of the nucleons in the target nucleus is taken into account using the algorithm in Ref. [26], and the energy-momentum conservation is enforced. We denote the initial momenta of the nucleons of the nucleus $A(B)$ as $(\sum_{i=1}^{A} p_{zi},\ \sum_{i=1}^{A} p_{Ti} = 0)$. The final momenta $(\sum_{i=1}^{A} p'_{zi},\ \sum_{i=1}^{A} p'_{Ti} = 0)$ are determined as follows. First we characterize, in the case of two nuclei A and B, the ith nucleon of the nucleus by the variables,

$$x_i^+ = \frac{E_i + p_{zi}}{W_A^+} \quad \text{and} \quad p_{Ti}, \tag{7}$$

and the jth nucleon of nucleus B by

$$y_j^- = \frac{E_j - q_{zj}}{W_B^-} \quad \text{and} \quad q_{Tj}, \tag{8}$$

where

$$W_A^+ = \sum_{i=1}^{A} (E_i + p_{zi}), \tag{9}$$

$$W_B^- = \sum_{j=1}^{B} (E_j - q_{zj}). \tag{10}$$

Here $E_i(E_j)$ and $p_{zi}(q_{zj})$ are the initial energy and longitudinal momentum of the ith (jth) nucleon. The corresponding total energy and momentum are given by $E^0 = \sum_{i=1}^{A} E_i$ and $p_z^0 = \sum_{i=1}^{A} p_{zi}$, respectively. The value of $x_i'^+(y_j'^-)$ is distributed according to the distribution,

$$P(x_i'^+) \propto \prod_{i=1}^{A} \exp -\left(\frac{(x_i'^+ - 1/A)^2}{d^2}\right), \tag{11}$$

where $d = 0.07$. This distribution is defined by fitting the average emission angle of evaporated singly and multiply charged nuclear fragments [26]. The value of $p'_{Ti}(q'_{Tj})$ is simulated according to

$$P(p'_{Ti}) \propto \prod_{i=1}^{A} \exp\left(-\frac{p_{Ti}'^2}{\langle p_T^2\rangle}\right), \tag{12}$$

where $\langle p_T^2\rangle = 0.07(\text{GeV}/c)^2$ [26]. The distributions (11) and (12) are calculated under the constraints $\sum_{i=1}^{A} p'_{Ti} = 0$ and $\sum_{i=1}^{A} x_i'^+ = 1$. The sum of transverse momenta gives the Fermi motion of nucleus $A(B)$.

(iii) After the collective cascade, the momentum of the ith (jth) nucleon is obtained in terms of $\{x_i'^+, p'_{Ti}\}$ and $\{y_j'^-, q'_{Tj}\}$,

$$p'_{zi} = \left(W_A'^+ x_i'^+ - \frac{m_{Ti}'^2}{x_i'^+ W_A'^+}\right)\Big/2, \tag{13}$$

$$q'_{zj} = -\left(W_B'^- y_j'^- - \frac{\mu_{Tj}'^2}{y_j'^- W_B'^-}\right)\Big/2, \tag{14}$$

where $\mu_{Tj}'^2 = m_i^2 + p_{Ti}'^2$, $\mu_{Tj}'^2 = \mu_j^2 + q_{Tj}'^2$, and $m_i(\mu_j)$ is the mass of the ith (jth) nucleon from $A(B)$.

In the expressions (13) and (14) $W_A'^+$ and $W_B'^-$ are calculated by applying the energy-momentum conservation,

$$\begin{aligned} \sum_{i=1}^{A} E'_i + \sum_{j=1}^{B} E'_j &= \frac{W_A'^+}{2} + \frac{1}{2W_A'^+}\sum_{i=1}^{A}\frac{m_{Ti}'^2}{x_i'^+} \\ &\quad + \frac{W_B'^-}{2} + \frac{1}{2W_B'^-}\sum_{j=1}^{B}\frac{\mu_{Tj}'^2}{y_j'^-} \\ &= E_A^0 + E_B^0, \end{aligned} \tag{15}$$

$$\sum_{i=1}^{A} p'_{zi} + \sum_{j=1}^{B} q'_{zj} = \frac{W'^{+}_{A}}{2} - \frac{1}{2W'^{+}_{A}} \sum_{i=1}^{A} \frac{m'^{2}_{Ti}}{x'^{+}_{i}} - \frac{W'^{-}_{B}}{2} + \frac{1}{2W'^{-}_{B}} \sum_{j=1}^{B} \frac{\mu'^{2}_{Tj}}{y'^{-}_{j}} = p^{0}_{zA} + q^{0}_{zB}, \quad (16)$$

and

$$\sum_{i=1}^{A} p'_{iT} + \sum_{j=1}^{B} q'_{Tj} = 0. \quad (17)$$

More explicitly, W'^{+}_{A} and W'^{-}_{B} are given by

$$W'^{+}_{A} = \frac{(W^{-}_{0} W^{+}_{0} + \alpha - \beta + \sqrt{\Delta})}{2W^{-}_{0}}, \quad (18)$$

$$W'^{-}_{B} = \frac{(W^{-}_{0} W^{+}_{0} - \alpha + \beta + \sqrt{\Delta})}{2W^{+}_{0}}, \quad (19)$$

where

$$W^{+}_{0} = (E^{0}_{A} + E^{0}_{B}) + (p^{0}_{zA} + q^{0}_{zB}),$$
$$W^{-}_{0} = (E^{0}_{A} + E^{0}_{B}) - (q^{0}_{zA} + q^{0}_{zB}),$$
$$\alpha = \sum_{i=1}^{A} \frac{m'^{2}_{Ti}}{x'^{+}_{i}}, \quad \beta = \sum_{j=1}^{B} \frac{\mu'^{2}_{Tj}}{y'^{-}_{j}},$$

and $\Delta = (W^{-}_{0} W^{+}_{0})^{2} + \alpha^{2} + \beta^{2} - 2W^{-}_{0} W^{+}_{0} \alpha - 2W^{-}_{0} W^{+}_{0} \beta - 2\alpha\beta$.

(iv) At a given impact parameter and given coordinates of the target nucleons (in the corresponding reference frame) one can determine the primary interacting or "wounded" nucleons of the nuclei according to the eikonal formalism as implemented in the HIJING.

(v) One has to look for all spectator nucleons of the target nucleus. If the ith spectator nucleon is at the impact-parameter distance $b_{ij} = |\vec{r}_i - \vec{r}_j|$ from the jth wounded nucleon, then it is considered to be a participant of the collision with a probability,

$$\varphi = C \ \exp\left(-b^{2}_{ij}/r^{2}_{c}\right), \quad (20)$$

where r_c is the mean interaction radius and C is a strength factor. In the present calculations, these values are fixed at $C = 1$ and $r_c = 1.2$ fm. Note that in the case of $C = 0$, φ reduces to the eikonal case, no cascading.

(vi) If the number of newly involved nucleons is not zero, then step (v) is repeated, otherwise step (vii) is carried out. This allows one to include 3,4,5,..., etc., nucleons in the interaction (see Fig. 1).

(vii) The momentum of the wounded nucleons (which are determined either from the eikonal formalism or the Regge cascading) are simulated using steps (ii) and (iii) by replacing $A(B)$ with the number of wounded nucleons of nucleus $N_{A(B)}$. Also, the values of d and $\langle p^{2}_{T} \rangle$ in Eqs. (10) and (11) are increased to 0.5 and 0.5 $(\mathrm{GeV}/c)^{2}$, respectively.

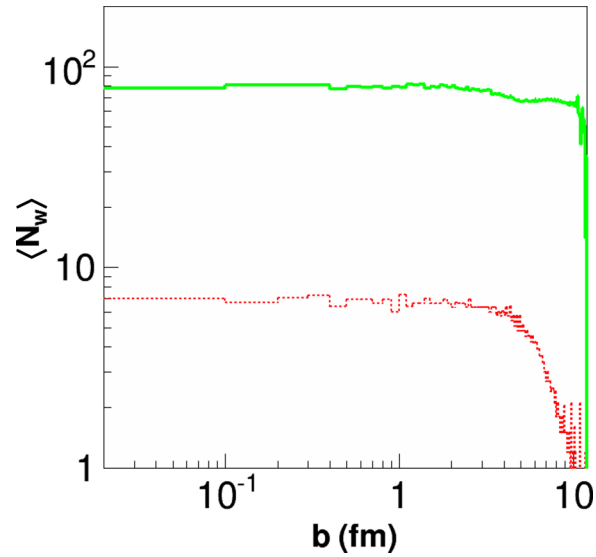

FIG. 2. (Color online) The average number of wounded nucleons N_w as a function of impact parameter (b). The solid and dotted lines denote the ImHIJING calculations with and without collective cascade, respectively.

In Fig. 2 we calculate the average number of wounded nucleons N_w as a function of impact parameter (b) for p + Pb collisions at $\sqrt{s_{\mathrm{NN}}} = 5.02$ TeV. As one can see, when $C = 0$ (no collective cascade) $N_w \approx 7$ in the impact-parameter interval $0 < b < 5$ fm, which gives the average number of primary interacting nucleons calculated in the eikonal formalism of the HIJING code. On the other hand, when $C = 1$ (full collective cascade), $N_w \approx 80$ in the range of $0 < b < 10$ fm, implying a large number of spectator nucleons that are involved in the collision process. As will be shown below, these spectator nucleons are used to induce a nuclear modification effect (shadowing) for nucleons that are involved in primary interactions inside the nucleus.

It is worthwhile mentioning that the implementation of the collective cascade in the FRITIOF model solves the problem of secondary interactions into the nucleus [13,14]. As shown in Ref. [14], the combined model reproduces rather well the proton and charged pion transverse momentum spectra (at $p_T \leqslant 1\mathrm{GeV}/c$) from p + Cu and Pb collisions at 3, 8, and 15 GeV/c.

In the numerical calculations, the HIJING model is run in two modes: the standard HIJING 1.383 with the DO1984 parametrizations (StdHIJING) and the ImHIJING, which incorporates the MSTW2009 PDFs. In what follows, we denote the ImHIJING calculations with and without Regge collective cascading as ImHIJING/CAS and ImHIJING/noCAS, respectively. In all calculations, the default HIJING 1.383 parameters are selected, and no jet quenching is assumed.

III. RESULTS AND DISCUSSION

In this section, we display the predictions of the ImHIJING (StdHIJING) code along with the recent measurements of charged particles' spectra in $p + p$ [27–31] and p + Pb [1,4,7] collisions at LHC energies. Because the charged particles'

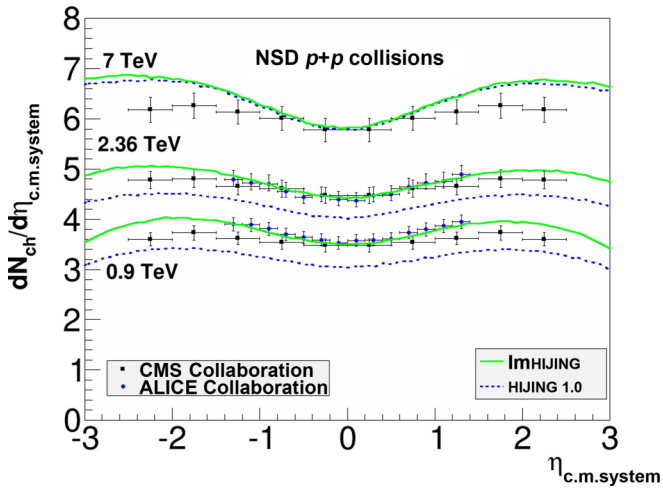

FIG. 3. (Color online) Pseudorapidity density of charged particles in NSD $p+p$ collisions at LHC energies as compared to the HIJING results. The experimental data are from the CMS Collaboration [29,30] and the ALICE Collaboration [27].

spectra in $p+\mathrm{Pb}$ collisions are measured in minimum bias, we generate 2×10^6 events for a range of impact parameters from 0 to $2R_A$, i.e., 20 000 events are generated in equally spaced 100 impact-parameter intervals. As was performed for experimental data, the analysis of the ImHIJING (StdHIJING) generated events exclude single diffractive collisions.

Let us first test the validity of the ImHIJING code in $p+p$ collisions at LHC energies. Shown in Figs. 3–5 are the results obtained by the ImHIJING and StdHIJING codes as compared to the CMS Collaboration measurements for NSD $p+p$ interactions at 0.9, 2.36, and 7 TeV in the larger pseudorapidity interval $|\eta_{\mathrm{c.m.system}}|<2.4$. The fits to the central pseudorapidity densities of the charged multiplicities ($dN_{\mathrm{ch}}/d\eta_{\mathrm{c.m.system}}\,|\eta_{\mathrm{c.m.system}=0}$) as the colliding energy increases are used to re-adjust the values of the cutoff p_0 in the ImHIJING. We find that the values of p_0 at 3.2, 4.5, and 6.0 GeV/c^2 give the best fit to $dN_{\mathrm{ch}}/d\eta_{\mathrm{c.m.system}}|_{\eta_{\mathrm{c.m.system}}=0}$ at colliding energies of 0.9, 2.36, and 7.0 TeV, respectively. As one can see, the ImHIJING gives the best description of the pseudorapidity densities, the multiplicity distributions of charged particles $P(N_{\mathrm{ch}})$, and transverse momentum spectra at all energies. In particular, the ImHIJING predicts the general trends of the $dN_{\mathrm{ch}}/d\eta_{\mathrm{c.m.system}}$ distributions; for a weak $\eta_{\mathrm{c.m.system}}$ dependent with a slow increase towards higher $\eta_{\mathrm{c.m.system}}$ values and then a decrease at $|\eta_{\mathrm{c.m.system}}|>2$ as the collision energy decreases, see Fig. 3. Notice that the ImHIJING results are more consistent with the ALICE Collaboration measurements and systematically above the CMS Collaboration data. The reduction in the CMS Collaboration pseudorapidity density measurements is likely related to the fact that the contributions from charged leptons were not counted as primary particles [29]. For $P(N_{\mathrm{ch}})$, see Fig. 4, the ImHIJING gives a very good description of the multiplicity distributions at all energies. It should be noted that HIJING 2.0 (using the GRV1995 parametrization of the PDFs) falls short of the experimental $P(N_{\mathrm{ch}})$ data at a high multiplicity tail ($N_{\mathrm{ch}}>25$), especially at $\sqrt{s}=7$ TeV [6]. Finally for the transverse momentum spectra, see Fig. 5, the ImHIJING gives the best description at all energies but tends to overestimate the spectra at 7 TeV when $p_T>4\,\mathrm{GeV}/c$.

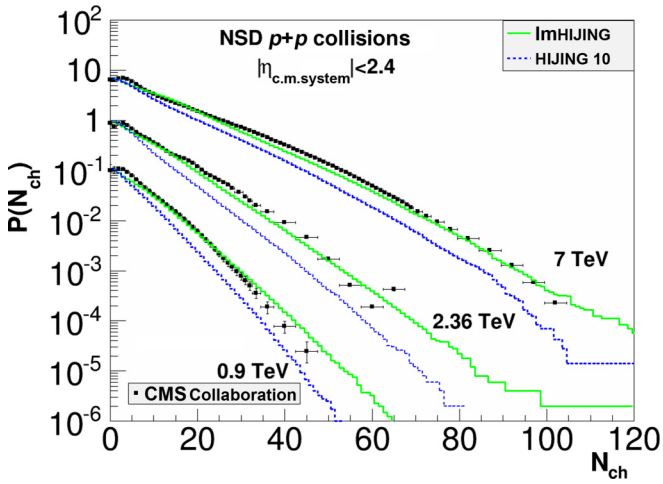

FIG. 4. (Color online) Multiplicity distributions of charged particles within $|\eta_{\mathrm{c.m.\ system}}|<2.4$ and $p_T>500\,\mathrm{MeV}/c$ in NSD $p+p$ collisions at LHC energies from the CMS Collaboration experiment [31] as compared to the HIJING results. For clarity, only the histograms and the data for the smaller energy are given in absolute values. The other ones have been multiplied by 10^1 and 10^2 for other energies in increasing order.

On the other hand, the StdHIJING produces lower charged particle densities (Fig. 3), too few charged particles (Fig. 4), and, finally, low transverse momentum (Fig. 5), especially for 0.9- and 2.36-TeV data. At 7 TeV, however, the StdHIJING is more consistent with the measured pseudorapidity densities and the transverse momentum spectra.

It should be noted that the ImHIJING results for the charged particle multiplicities are compatible with those from modern hard-scattering models [31], such as the PYTHIA 6 [32] event generator tuned to the CDF Collaboration data (PYTHIA D6T) and the new fragmentation model of PYTHIA 8 [33]. However, PYTHIA D62 and PYTHIA 8 significantly underestimate the pseudorapidity densities [27].

Next, in Figs. 6–8, we compare both the ImHIJING/CAS(noCAS) and the StdHIJING results with the global observables of charged particles for NSD $p+\mathrm{Pb}$ collisions at $\sqrt{s_{\mathrm{NN}}}=5.02$ TeV. The cutoff parameter is fixed at $p_0=5.4\,\mathrm{GeV}/c$ where we use Eq. (3) for $p+p$ collisions at $\sqrt{s_{\mathrm{NN}}}=5.02$ TeV. The StdHIJING calculations are with a constant cutoff parameter $p_0=2\,\mathrm{GeV}/c$ and a parton shadowing parameter of $\alpha_{q(g)}=0.1$.

In Fig. 6 we investigate the charged particle density in the laboratory system $dN_{\mathrm{ch}}/d\eta_{\mathrm{lab}}$. As was performed for the ALICE Collaboration experiment [7], both ImHIJING/Sc(noSc) and StdHIJING calculations assume that the proton is moving in the negative z direction at 4-TeV energy, whereas the Pb ion is moving in the positive z direction at (82×)-TeV energy. It is interesting to note that the effect of collective cascading increases when going from proton ($\eta_{\mathrm{lab}}\approx-1.4$) to Pb ($\eta_{\mathrm{lab}}\approx3.4$) peak regions. The ImHIJING/CAS results (thick line) lead to a better agreement with the data and can predict the forward-backward asymmetry shape of $dN_{\mathrm{ch}}/d\eta_{\mathrm{lab}}$.

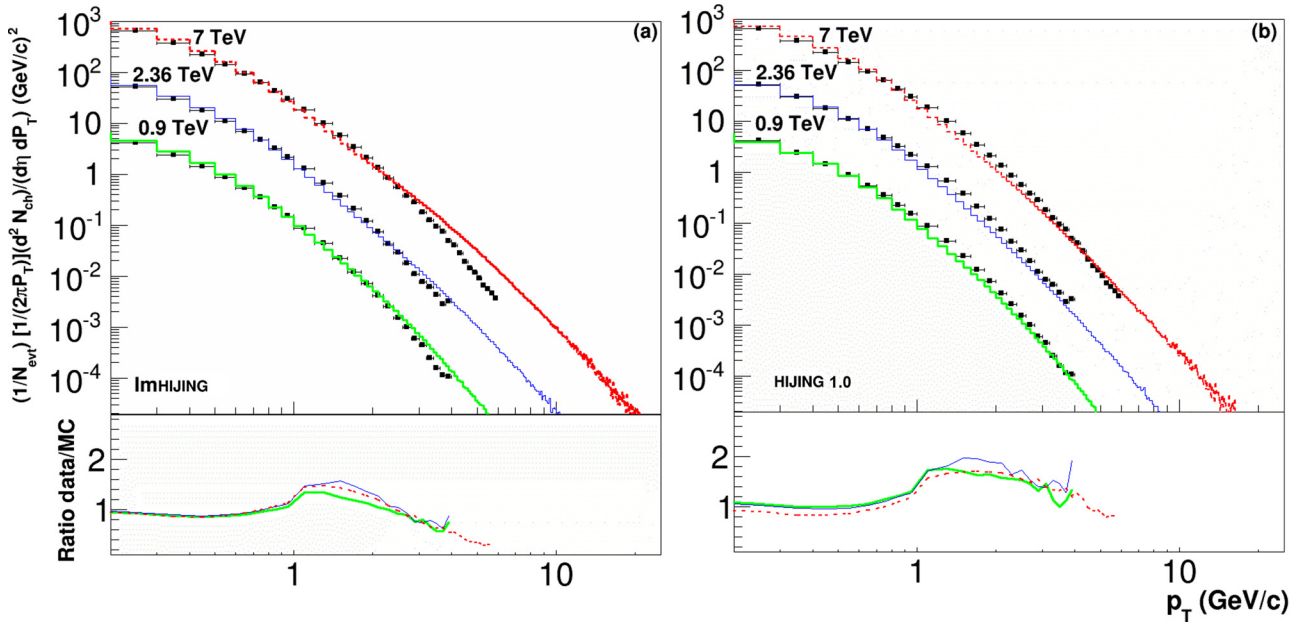

FIG. 5. (Color online) Transverse momentum distributions of charged particles in the range of $|\eta_{\text{c.m. system}}| < 2.4$ in NSD $p + p$ collisions at LHC energies as compared to the HIJING results. The square points with error bars denote the CMS Collaboration experimental data [29,30]. For clarity, only the histograms and the data for the smaller energy are given in absolute values. The other ones have been multiplied by 10^1 and 10^2 for other energies in increasing order. (a) and (b) are the results calculated by the ImHIJING and HIJING 1.0, respectively. For both cases the ratios between the measured values and the Monte Carlo (MC) HIJING calculations are shown in the lower part with the same convention.

Figure 6 also shows that the default StdHIJING describes the trend seen in the data, although it seems that with the soft shadowing parameter $\alpha_{q(g)} = 0.1$ the model underpredicts the data. On the other hand, the HIJING 2.1 model [15] with the GRV1995 parametrizations and gluon shadowing ($\alpha_g = 0.2$) constrained from $dN_{\text{ch}}/d\eta_{\text{c.m. system}}$ data in $d + \text{Au}$ collisions at $\sqrt{s_{\text{NN}}} = 0.2\,\text{TeV}$ agree with the measured pseudorapidity density, except for an overestimation in the proton peak region [7].

In Fig. 7 we examine the p_T spectra of charged particles in the central ($|\eta_{\text{c.m.system}}| < 0.3$) and backward ($-0.8 < \eta_{\text{c.m.system}} < -0.3$ and $-1.3 < \eta_{\text{c.m.system}} < -0.8$) pseudorapidity ranges. It is pointed out in Refs. [1,4] that at high p_T, the measured p_T spectrum of charged particles in $p + \text{Pb}$ collisions is similar to those in interpolated $p + p$ reference spectra at $|\eta_{\text{c.m.system}}| < 0.3$, obtained by scaling data measured at $\sqrt{s_{\text{NN}}} = 2.76$ and 7 TeV. As one can see, the ImHIJING calculated $p + p$ reference spectra agree with the measured $p + \text{Pb}$ spectra at high p_T ($p_T > 6\,\text{GeV}/c$). This may imply that the ImHIJING initial conditions for PDFs are consistent with the data at $\sqrt{s_{\text{NN}}} = 5.02\,\text{TeV}$.

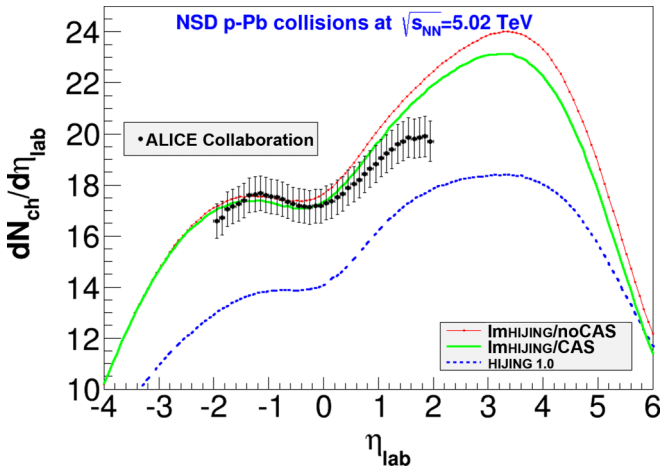

FIG. 6. (Color online) Pseudorapidity density (in the laboratory system) of charged particles in NSD $p + \text{Pb}$ collisions at $\sqrt{s_{\text{NN}}} = 5.02\,\text{TeV}$ from the ALICE Collaboration experiment [7] as compared to the improved HIJING results.

In the region of low p_T spectra ($p_T < 6\,\text{GeV}/c$) one thus can quantify nuclear effects in $p + \text{Pb}$ collisions at the specified pseudorapidity intervals. However, Fig. 7 demonstrates that there is almost no difference between the ImHIJING/CAS and the ImHIJING/noCAS results for the whole p_T spectra in all pseudorapidity ranges. It can also be observed that the ImHIJING/CAS(noCAS) calculations agree with the corresponding experimental data at $p_T < 6\,\text{GeV}/c$. Starting from $p_T > 6\,\text{GeV}/c$, the ImHIJING/CAS(noCAS), however, overestimates both the calculated $p + p$ reference and the measured data, which indicates that the HIJING implementation of final-state interactions in a dense medium is not well accounted for.

On the other hand, calculations with the default StdHIJING, see Fig. 8, are a good fit for both low $p_T < 1\,\text{GeV}/c$ and high ($p_T > 6\,\text{GeV}/c$) p_T-charged particles in $p + \text{Pb}$ collisions. However, the StdHIJING calculated $p + p$ reference spectra underestimate the measured high p_T distributions in $p + \text{Pb}$ collisions. This indicates that the StdHIJING calculations are not consistent with the measured p_T spectra of charged particles.

Finally, the systematic difference between the ImHIJING/CAS(noCAS) results and the data for the p_T

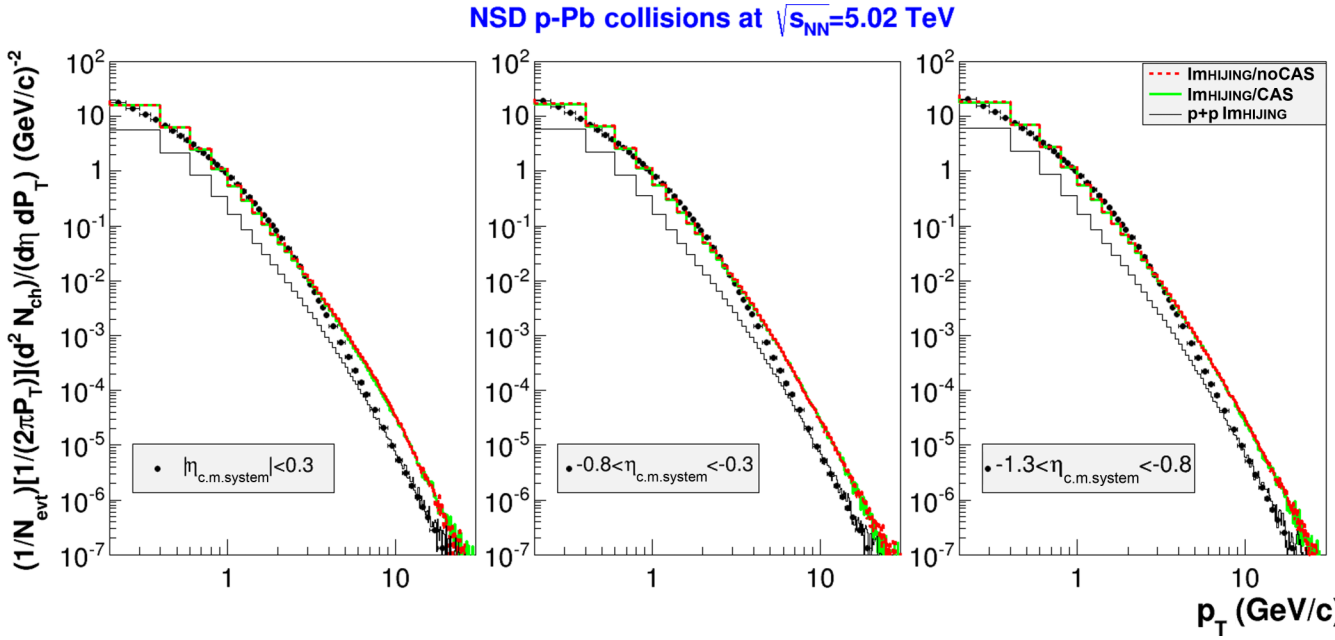

FIG. 7. (Color online) Transverse momentum distributions of charged particles at different pseudorapity intervals in NSD $p+$Pb collisions at $\sqrt{s_{\rm NN}} = 5.02$ TeV from the ALICE Collaboration experiment [1,4] as compared to the improved HIJING results.

spectra are illustrated in Fig. 9 where we compare the experimental p_T-differential yield in $p+$Pb relative to the $p+p$ reference with the ImHIJING/CAS and the ImHIJING/noCAS at the central ($|\eta_{\rm c.m.system}| < 0.3$) and whole ($-1.3 < \eta_{\rm c.m.system} < 0.3$) pseudorapidity ranges. The nuclear modification factor is calculated as

$$R_{p\rm Pb} = \frac{d^2N_{\rm ch}^{p\rm Pb}\Big/d\eta\, d p_T}{\langle N_{\rm coll}\rangle d^2N_{\rm ch}^{pp}\Big/d\eta\, d p_T}, \qquad (21)$$

where $\langle N_{\rm coll}\rangle$ is the average number of collisions. As one can see, at low $p_T < 8\,{\rm GeV}/c$ reduced emission of charged particles is observed in the ImHIJING/CAS compared to the ImHIJING/noCAS, which leads to a better agreement with the data. At $p_T > 6\,{\rm GeV}/c$, the ImHIJING/CAS(noCAS) calculations of $R_{p\rm Pb}$ are consistent with unity, demonstrating a strong suppression of $p+$Pb to $p+p$ collisions. It should be pointed out that the ImHIJING/CAS results for $p_T > 6$ are compatible with those of Helenius *et al.*, performed with shadowing calculations and global EPS09s PDFs [34].

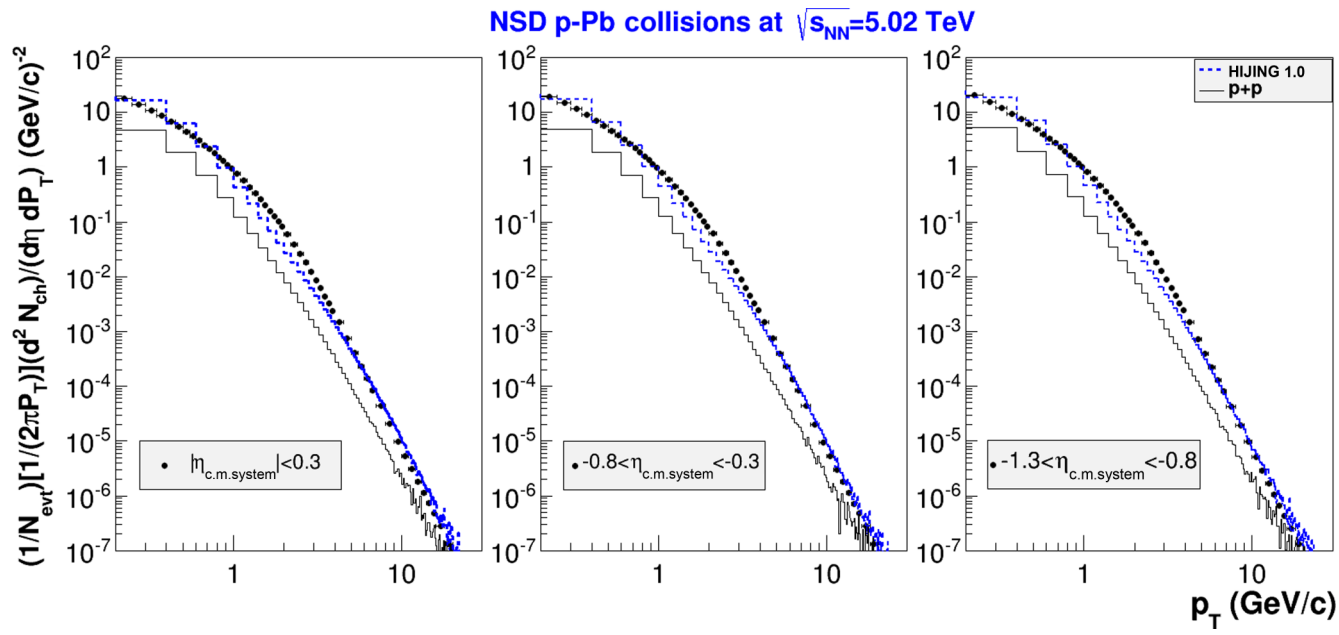

FIG. 8. (Color online) The same as Fig. 7, but here the lines denote the standard HIJING calculations.

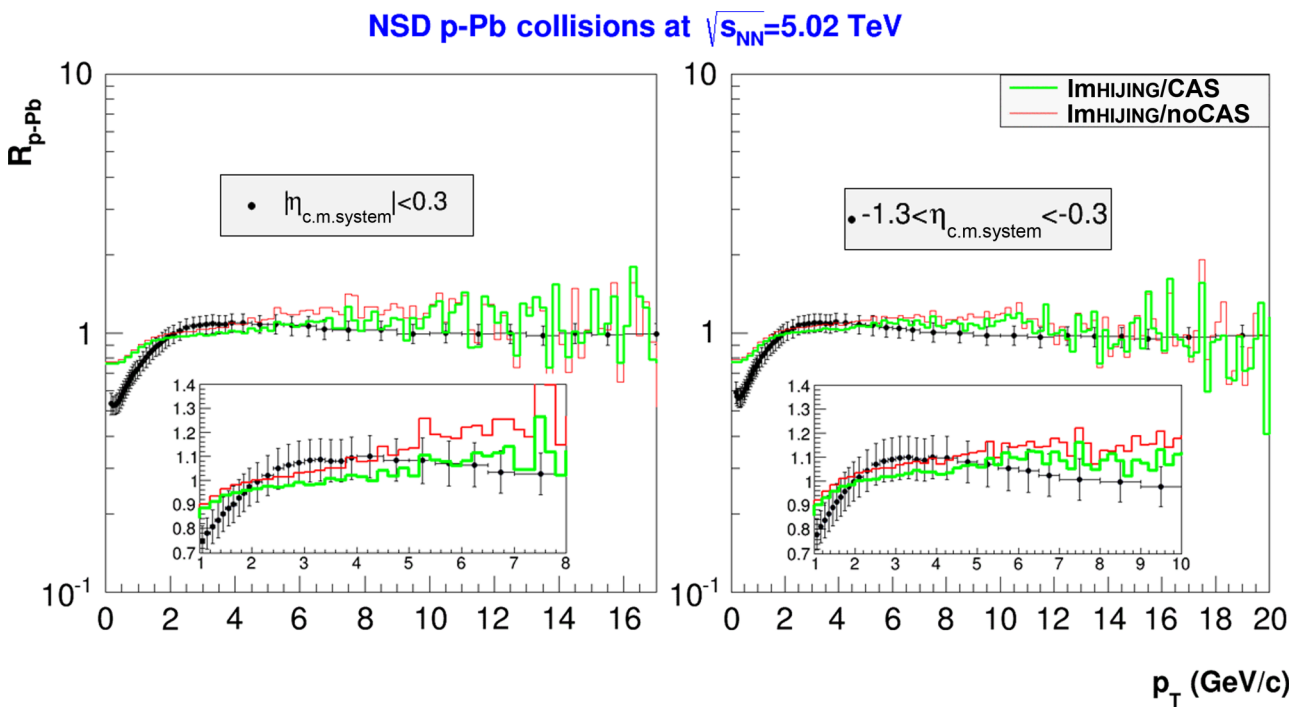

FIG. 9. (Color online) Transverse momentum dependence of the nuclear modification factor of charged particles at different pseudorapity intervals in NSD $p+$Pb collisions at $\sqrt{s_{\rm NN}} = 5.02$ TeV from the ALICE Collaboration experiment [1,4] as compared to the improved HIJING results. The insets show a closeup of the region where the effect of the collective cascade is more pronounced.

The StdHIJING calculations (not shown here), which predict well the p_T spectra of charged particles, underpredict the $R_{p\rm Pb}$ values. It is worth noting that the StdHIJING results are similar to those of HIJING 2.1 [15] using the GRV1995 PDFs with parton shadowing of strength $\alpha_g = 0.28$ [1]. This may imply that the nuclear modification data of NSD $p+$Pb collisions at $\sqrt{s_{\rm NN}} = 5.02$ TeV provide important constraints to HIJING-type models.

In conclusion, it can be stated that the description of charged particles' spectra in $p+p$ and Pb collisions at LHC energies depends strongly on the detailed description of the initial conditions which combines both the proper PDFs and a collective cascade as can be achieved in the ImHIJING/CAS calculation.

IV. SUMMARY AND CONCLUSIONS

A comparison of the recently measured data of NSD $p+p$ and Pb collisions at LHC energies is presented in the framework of an improved HIJING (ImHIJING/CAS) model. Compared to the StdHIJING model, this improved version includes the recent MSTW2009 parton distribution functions determined from global analysis of hard-scattering data and a collective cascade picture which accounts for a cascade on the plane of the impact parameter. From the calculation results one can draw the following conclusions:

(i) The StdHIJING (that with the DO1984 PDFs) calculation can describe the transverse momentum spectra of NSD $p+p$ collisions at $\sqrt{s} = 0.9$, 2.36, and 7 TeV but tends to underestimate both the pseudorapidity densities (except for the measurements at 7 TeV) and the multiplicity distributions of charged particles within $|\eta_{\rm c.m.system}| < 2.4$.

(ii) The ImHIJING (that with the MSTW2009 PDFs) calculation reproduces rather well the measured charged particles in NSD $p+p$ collisions at LHC energies.

(iii) The StdHIJING (that with parton shadowing) calculation can predict well the p_T spectra of charged particles in NSD $p+$Pb collisions at $\sqrt{s_{\rm NN}} = 5.02$ TeV but underpredict both the measured nuclear modification factor and the pseudorapidity density.

(iv) The ImHIJING/CAS (that with the collective cascade) calculation is a good fit to the charged particles spectra in NSD $p+$Pb collisions. Only for the transverse momentum distributions at $p_T > 6\,{\rm GeV}/c$ are the charged particles' spectra overpredicted.

(v) Some effects of the collective cascade are found on the pseudorapidity density of NSD $p+$Pb collisions: The effect of collective cascading increases when going from proton ($\eta_{\rm lab} \approx -1.4$) to Pb ($\eta_{\rm lab} \approx 3.4$) peak regions.

(vi) In contrast to the p_T distributions, the transverse momentum dependence of the nuclear modification factor of charged particles in NSD $p+$Pb collisions at $1 < p_T < 8\,{\rm GeV}/c$ is found to be sensitive to the collective cascade, especially in the central pseudorapidity interval $|\eta_{\rm c.m.system}| < 0.3$.

Thus, the implantation of proper PDFs and a collective cascade picture in the HIJING is of importance for the description of the charged particles' spectra in $p+p$ and

Pb collisions at LHC energies. We expect that the collective cascade picture will play an essential role for the description of more massive systems, e.g., the charged particles' spectra in NSD Pb + Pb collisions at $\sqrt{s_{\rm NN}} = 2.76$ TeV [2]. This work is in progress.

ACKNOWLEDGMENTS

The authors would like to thank Professor V. V. Uzhinskii for checking the IMHIJING/CAS code. K.A.-W. would like to thank the members of the GEANT4 hadronic group for hospitality and advice during his visits to CERN.

[1] B. Abelev *et al.* (ALICE Collaboration), Phys. Rev. Lett. **110**, 082302 (2013).
[2] B. Abelev *et al.* (ALICE Collaboration), Phys. Lett. B **720**, 52 (2013).
[3] B. Abelev *et al.* (ALICE Collaboration), Phys. Lett. B **727**, 371 (2013).
[4] B. Abelev *et al.* (ALICE Collaboration), Eur. Phys. J. C **74**, 3054 (2014).
[5] X.-N. Wang and M. Gyulassy, Phys. Rev. Lett. **68**, 1480 (1992); Phys. Rev. D **44**, 3501 (1991).
[6] W.-T. Deng, X.-N. Wang, and R. Xu, Phys. Rev. C **83**, 014915 (2011); Phys. Lett. B **701**, 133 (2011).
[7] B. Abelev *et al.* (ALICE Collaboration), Phys. Rev. Lett. **110**, 032301 (2013).
[8] M. Gluck, E. Reya, and A. Vogt, Z. Phys. C **67**, 433 (1995).
[9] A. D. Martin, W. J. Stirling, R. S. Thorne, and G. Watt, Eur. Phys. J. C **63**, 189 (2009).
[10] K. Abdel-Waged and V. V. Uzhinskii, Phys. At. Nucl. **60**, 828 (1997).
[11] K. Abdel-Waged and V. V. Uzhinskii, J. Phys. G: Nucl. Part. Phys. **24**, 1723 (1998).
[12] B. Andersson, G. Gustafson, and B. Nilsson-Almqvist, Nucl. Phys. B **281**, 289 (1987); B. Nillsson-Almquist and E. Stenlund, Comput. Phys. Commun. **43**, 387 (1987).
[13] K. Abdel-Waged, Phys. Rev. C **59**, 2792 (1999).
[14] K. Abdel-Waged, N. Felemban, and V. V. Uzhinskii, Phys. Rev. C **84**, 014905 (2011).
[15] R. Xu, W.-T. Deng, and X.-N. Wang, Phys. Rev. C **86**, 051901 (2012).
[16] V. Topor Pop, M. Gyulassy, J. Barrette, C. Gale, and A. Warburton, Phys. Rev. C **86**, 044902 (2012).
[17] T. Sjöstrand and M. van Zijl, Phys. Rev. D **36**, 2019 (1987).
[18] A. Capella, U. Sukhatme, and J. Tran Thanh Van, Z. Phys. C **3**, 329 (1979).
[19] J. Ranft, Phys. Rev. D **37**, 1842 (1988).
[20] D. W. Duke and J. F. Owens, Phys. Rev. D **30**, 49 (1984).
[21] A. Abulencia *et al.* (CDF-Run II Collaboration), Phys. Rev. D **75**, 092006 (2007).
[22] T. Aaltonen *et al.* (CDF Collaboration), Phys. Rev. D **78**, 052006 (2008).
[23] V. M. Abazov *et al.* (DØ Collaboration), Phys. Rev. Lett. **101**, 062001 (2008).
[24] G. Aad *et al.* (ATLAS Collaboration), Nucl. Phys. B **889**, 486 (2014); and references therein.
[25] G. Antchev *et al.* (TOTEM Collaboration), Europhys. Lett. **96**, 21002 (2011).
[26] M. I. Adamovich *et al.* (EMU01 Collaboration), Z. Phys. A: Hadrons Nucl. **358**, 337 (1997).
[27] K. Aamodt *et al.* (ALICE Collaboration), Eur. Phys. J. C **68**, 89 (2010).
[28] K. Aamodt *et al.* (ALICE Collaboration), Eur. Phys. J. C **68**, 345 (2010).
[29] V. Khachatryan *et al.* (CMS Collaboration), J. High Energy Phys. 02 (2010) 041.
[30] V. Khachatryan *et al.* (CMS Collaboration), Phys. Rev. Lett. **105**, 022002 (2010).
[31] V. Khachatryan *et al.* (CMS Collaboration), J. High Energy Phys. 01 (2011) 079.
[32] M. G. Albrow *et al.* (Tevatron-for-LHC QCD Working Group), arXiv:hep-ph/0610012.
[33] T. Sjostrand, S. Mrenna, and P. Z. S. Kands, Comput. Phys. Commun. **178**, 852 (2008).
[34] I. Helenius, K. J. Eskola, H. Honkanen, and C. A. Sagado, J. High Energy Phys. 07 (2012) 073.